Partitioning of Oleic Acid into Phosphatidylcholine Membranes Is Amplified by Strain

ARTICLE *in* THE JOURNAL OF PHYSICAL CHEMISTRY B · SEPTEMBER 2013

Impact Factor: 3.3 · DOI: 10.1021/jp404135g · Source: PubMed

3 AUTHORS:

Mojca Mally
University of Ljubljana
5 PUBLICATIONS **89** CITATIONS
SEE PROFILE

Primož Peterlin
Institute of Oncology Ljubljana
21 PUBLICATIONS **230** CITATIONS
SEE PROFILE

Saša Svetina
University of Ljubljana
132 PUBLICATIONS **2,297** CITATIONS
SEE PROFILE

THE JOURNAL OF PHYSICAL CHEMISTRY B

Article

pubs.acs.org/JPCB

Partitioning of Oleic Acid into Phosphatidylcholine Membranes Is Amplified by Strain

Mojca Mally,*[,†] Primož Peterlin,[†,‡] and Saša Svetina[†,§]

[†]Institute of Biophysics, Faculty of Medicine, University of Ljubljana, Slovenia, 1000 Ljubljana, Slovenia

[‡]Institute of Oncology, 1000 Ljubljana, Slovenia

[§]Jožef Stefan Institute, 1000 Ljubljana, Slovenia

ABSTRACT: Partitioning of fatty acids into phospholipid membranes is studied on giant unilamellar vesicles (GUVs) utilizing phase-contrast microscopy. With use of a micropipet, an individual GUV is transferred from a vesicle suspension in a mixed glucose/sucrose solution into an isomolar glycerol solution with a small amount of oleic acid added. Oleic acid molecules intercalate into the phospholipid membrane and thus increase the membrane area, while glycerol permeates into the vesicle interior and thus via osmotic inflation causes an increase of the vesicle volume. The conditions are chosen at which a vesicle swells as a sphere. At sufficiently low oleic acid concentrations, when the critical membrane strain is reached, the membrane bursts and part of vesicle content is ejected, upon which the membrane reseals and the swelling commences again. The radius of the vesicle before and after the burst is determined at different concentrations of oleic acid in suspension. The results of our experiments show that the oleic acid partitioning increases when the membrane strain is increased. The observed behavior is interpreted on the basis of a tension-dependent intercalation of oleic acid into the membrane.

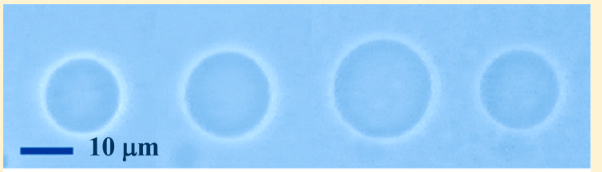

1. INTRODUCTION

Partitioning of free fatty acids (FFAs) into phospholipid membranes is the first step in transmembrane transport of FFAs and has been thoroughly studied (reviewed in McArthur et al.[1]). Mixed phospholipid/fatty acid systems are also model systems for studying vesicle growth and replication.[2,3] In different experimental setups it has been shown that the integration of fatty acid (FA) molecules into the lipid membranes leads to growth and morphological changes of the membrane, which in certain conditions result in budding and division of vesicles (as reviewed in Hanczyc and Szostak[4]). These morphological processes are thought to be among the key steps of the early evolution of cellular life and have been shown to be remarkably similar to the proliferation of the L-form cells.[5,6] The significance of the FA concentration has been addressed in studying the morphological outcomes of FA-to-membrane lipid interactions: at low concentrations the "50 and 100 nm vesicles" swell, while at large concentrations the behavior of the vesicles is more complicated, but the results can still be interpreted within the concept of the mixed phospholipid/fatty acid vesicles growing both in size and in number.[7]

The FFA transport is affected by the size of the vesicle (i.e., by the membrane curvature) as the transport rates decrease with increasing vesicle radius,[8] and also by the size of the partitioning molecules: it has been shown by means of titration calorimetry that the partition coefficient of different FFAs into phospholipid membranes increases with the length of the hydrophobic tail.[9] Investigating the partitioning of different FFAs into Langmuir monolayers, it was found that saturated FAs make the membrane more rigid, while the presence of unsaturated FAs increases its fluidity,[10] thus indicating the role of the type of the partitioning molecules. It was established that FA partitioning into the membrane is rapid compared to flip-flop between the membrane leaflets.[8] However, the details of FFA interaction with the membrane are not yet fully understood and there is a persistent debate on the mechanisms enabling the FFA molecules to enter the cell.[11,12] To deepen our understanding of the FFAs partitioning into phospholipid membranes and the corresponding vesicle growth we have previously designed a study on giant phospholipid vesicles that can be monitored optically and continuously during their exposure to the solution of oleic acid (OA).[13] The experimental setup enabled an insight into the behavior of the vesicles which undergo a rapid increase in surface area and transform morphologically, but the vesicles with constant volume attain shapes with numerous protuberances and it was therefore difficult to quantify the surface area increase and to define the parameters that describe the interaction of OA with the vesicle membrane.

One of the technical issues that have to be addressed to allow for a quantitative analysis of the vesicle growth is to maintain the geometry of the vesicle simple enough. In some earlier studies where the interaction of phospholipid GUVs with bile

Received: April 26, 2013
Revised: August 29, 2013

   dx.doi.org/10.1021/jp404135g | J. Phys. Chem. B XXXX, XXX, XXX−XXX

acids[14] or lysolipids[15] was studied, micropipet aspiration has been used to sustain a simple geometrical shape of the vesicles. The present study was designed to allow for a simultaneous increase of vesicle volume and vesicle membrane area while keeping the vesicles spherical. Individual vesicles with encapsulated sucrose solution were brought into an environment that contained both glycerol and oleic acid. The phospholipid vesicle membrane is permeable for glycerol, which passes from the external solution through the membrane into the vesicle. The osmotic drag couples the inflow of glycerol with the inflow of water, causing the vesicle to swell, while the oleic acid from the external solution increases the membrane surface area by incorporating into the membrane. The flip-flop of oleic acid between the two membrane leaflets is fast with respect to the changes in the membrane stretching due to glycerol permeation, and at the chosen experimental conditions the vesicles maintained spherical shape throughout the experiment, which allowed us to measure their radius and determine the membrane area changes with great precision. It was established that in these conditions at low OA concentrations (under 0.1 mM) vesicles undergo a series of cyclic changes. In each cycle the radius of the vesicle gradually increases until the critical membrane strain is reached. At that point, the membrane bursts and part of the inner solution is ejected, upon which the radius abruptly returns to its initial value, the membrane reseals, and a new cycle begins.

The outline of this paper is as follows: first we present the experiments and the observations of the vesicle behavior; second, the various aspects of OA/vesicles interactions are considered and the results of the experiment are interpreted within the frame of a model for a membrane-strain-dependent OA intercalation into the membrane; third, the dynamics of the observed morphology changes is explained as a consequence of the osmotic process based on the glycerol permeation, and the membrane permeability for glycerol is estimated.

2. EXPERIMENTAL METHODS

2.1. Materials. Vesicle membranes were made from phosphatidylcholine (either 1-palmitoyl-2-oleoyl-*sn*-glycero-3-phosphocholine, POPC, or 1-stearoyl-2-oleoyl-*sn*-glycero-3-phosphocholine, SOPC; both obtained as powder from Avanti Polar Lipids Inc., Alabaster, AL, USA). In the text both types of vesicles are referred to as phosphatidylcholine (PC) GUVs unless specification is needed. The powder was dissolved in a 2:1 (v/v) mixture of chloroform and methanol to 1 mg/mL and stored at −15 °C. Anhydrous, pro analysi (p.a.) glucose and p.a. sucrose, oleic acid, and anhydrous glycerol (Fluka BioChemica, Buchs, Switzerland) were used without further purification. All the solutions were buffered at pH 8.8 with Trizma buffer (Trizma base and Trizma hydrochloride) to 5 mM final buffer concentration. Buffer components were obtained from Sigma Chemical Co. (St. Louis, MO, USA).

2.2. Methods. Phospholipid GUVs were prepared by the electroformation method[16] slightly modified. In brief, two Pt electrodes with a dry lipid film were placed into an electroformation chamber and filled with 0.2 M sucrose. An AC voltage (4 V/10 Hz) was applied for 2 h. In the next steps the voltage and the frequency were reduced to the final values of 1 V/1 Hz. The chamber was then drained and flushed with a buffered 0.2 M glucose solution, yielding a suspension of GUVs in a sucrose/glucose solution. The vesicles produced this way are mostly unilamellar and spherical, with diameters ranging from 10 to 100 μm. Prior to use, the prepared suspension was stored in a sealed test tube at room temperature for a maximum of 4 days. The procedure of vesicle preparation and the experimental equipment for vesicle manipulation and observation is described in detail in Mally et al.[17]

The osmolalities of sucrose, glucose, and OA/glycerol solutions were measured and the results showed that the solutions were 200 ± 3 mOsm; the deviations are thus in the range of the accuracy of the osmometer (1% of the measured value). In the control experiments we ascertained that milliosmolal differences of the solutions do not induce any changes on the observed vesicle (as for example in its shape or composition of its inner solution) and that the solutions can be considered isoosmolar.

2.3. Experimental Procedure. Phospholipid GUVs containing 0.2 M sucrose solution sink to the bottom of the experimental chamber due to the greater specific gravity of the sucrose solution compared to that of the surrounding solution, which also enables the image contrast with the inverted phase-contrast microscope to be improved.[18] Vesicles were selected one at a time by using the criteria that they had no visible protuberances and appeared unilamellar. The chosen vesicle was fully aspirated into a micropipet filled with glucose solution, and transferred into a chamber filled with 0.2 M glycerol solution containing OA (pH 8.8) at a given concentration. As the volume of the chamber vastly exceeds the volume of the vesicle, the amount of OA that binds to the vesicle does not significantly alter the concentration of OA in the experimental chamber, which can thus be treated as constant. All experiments were carried out at room temperature (25 ± 2 °C).

In cases where the vesicle did not fluctuate, its shape was approximated by a sphere. In the recorded image, the location of vesicle boundary was determined by the maximal gradient of image intensity (gray level).[19] From the measured radius of the vesicle cross section, the surface area of a spherical vesicle membrane was calculated.

3. RESULTS

3.1. The Experiment. After the transfer of individual GUVs from a mixed sucrose/glucose solution into an isomolar glycerol solution with OA added, the vesicles are observed to grow in size. Vesicles are swelling due to permeation of glycerol (initially present only in the external solution), accompanied by the osmotic drag of water.

Figure 1 shows the radii of the vesicle's cross sections for four vesicles upon their transfer into glycerol solution with 0.05−0.20 mM OA added. At these concentrations the vesicles grow for 20 min or more, doubling their radii in the process. The rate of the vesicle radius increase does not suggest any dependence on the OA concentration.

A different phenomenon was observed at lower OA concentrations: a vesicle grows to a certain size and then bursts, ejecting part of its interior (Figure 2). Typical time of the burst (opening and resealing of the membrane) is about 0.1 s. Upon burst, the vesicle membrane is able to reseal in most cases and the vesicle is spherical again, having approximately the same radius as at the beginning of the experiment (i.e., shortly after the transfer with the micropipet), and the process of growing, bursting, and resealing of the membrane repeats itself (Figure 3). The time intervals between the bursts are much longer (order of minutes) than the duration of the bursts.

Just before and immediately after the bursts, the radius of each vesicle was measured to determine the membrane area

dx.doi.org/10.1021/jp404135g | J. Phys. Chem. B XXXX, XXX, XXX−XXX

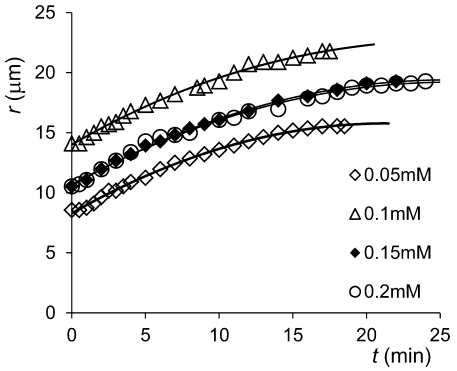

Figure 1. The increase of the vesicle radius r after the transfer of an individual POPC GUV from 0.2 M sugar solution into an isomolar solution of glycerol with different concentrations of OA added (as denoted in the legend). Four vesicles are shown to illustrate that the rate of the vesicle swelling does not depend on the OA concentration. The corresponding solid lines are best-fit curves, obtained by a fitting of a model prediction for the vesicle swelling (next section, eq 11) to data points, yielding the estimates for the membrane permeability for glycerol to be in the interval 1.9×10^{-8} m/s < P < 3.5×10^{-8} m/s.

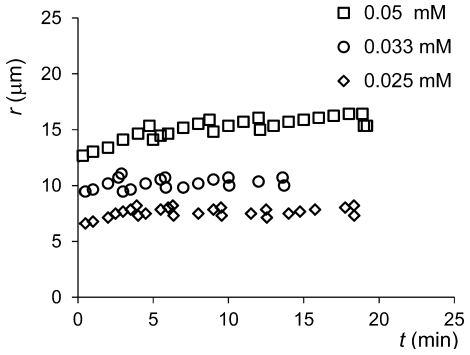

Figure 3. The periodical bursting of the vesicle at different OA concentrations (as denoted in the legend). Three of the POPC vesicles (from 28 successful experiments with POPC and 31 experiments with SOPC vesicles) are shown in this here to illustrate the process of swelling and bursting of the individual vesicle.

increase (characterized as the ratio between the membrane area before and after the burst) at different OA concentrations (Figure 4). The apparent relative dilation of vesicle membrane appears to increase with increasing OA concentration, ranging from a few percent in the transfer of GUVs into a glycerol solution completely devoid of OA[20] to ~100% in transfers into OA concentrations of 0.1 mM and above.

3.2. Analysis of the Results. Two distinct features are analyzed from a set of recorded transfers of PC GUVs into an isomolar glycerol solution with a small amount of OA added. First, the experimentally determined membrane area increase with respect to the concentration of OA in the solution is interpreted by a theoretical model (Figure 4). Second, membrane permeability for glycerol is estimated from the rate of vesicle swelling (Figure 1). Both results are then combined to relate the observed time elapsed between two successive bursts with the concentration of OA in the solution.

3.2.1. The Membrane Area at Vesicle Burst Depends on the Concentration of Oleic Acid in the Suspension. The observed vesicle bursting can be interpreted by using a model for tension-dependent intercalation of oleic acid molecules into the membrane. The critical aggregation concentration (cac) for single-chain amphiphiles like fatty acids has been reported to be in the range from 10^{-5} to 10^{-3} M;[2,21,22] specifically, with the experimental conditions analogous to our system, the cac value is estimated to be ~5×10^{-4} M.[2,13] Considering the corresponding value for phospholipids (~10^{-10} M),[23] the system can be treated as composed of two phases (membrane and suspension), with the insoluble phospholipid molecules present in the membrane-embedded phase only, while the fatty acid molecules and the oleate ions as more soluble components partition between the aqueous suspension and the membrane. Since the changes in the volume of the vesicle related to glycerol permeation occur on the time scale of 10^2 s, while all the fatty acid traffic (association, dissociation, and translocation) is much faster,[24] we can assume that fatty acid equilibrates between the two membrane leaflets, and thus we can neglect the effects related to the bilayer nature of the membrane. Stretching the membrane, (e.g., due to the osmotic inflation, as in the experiment described), however, induces partitioning of additional fatty acid into the membrane. The incorporated fatty acid molecules make the surface area of the relaxed membrane larger, thus reducing the difference between the actual (strained) membrane area and its relaxed value, and causing a favorable decrease of the elastic energy.

To deduce the relevant mechanisms that govern the behavior of the described system we formulate a model where the thermodynamic equilibrium of the system can be determined. The Gibbs free energy of the membrane can be written as the sum of the terms describing both the mixing of the two components and the membrane stretching caused by the glycerol-induced water flow into the vesicle interior:

$$G = H - TS + \frac{\kappa(A - \widetilde{A}_0)^2}{2\widetilde{A}_0} \quad (1)$$

where H is the enthalpy and S the entropy of the system at temperature T, κ is the area expansivity modulus, A is the actual (stretched) area of vesicle membrane, and $\tilde{A}_0$ is the relaxed membrane area with intercalated OA molecules. The area $\tilde{A}_0$ can be written as $\tilde{A}_0 = N_1a_1 + N_2a_2$, where N_1 and N_2 are the

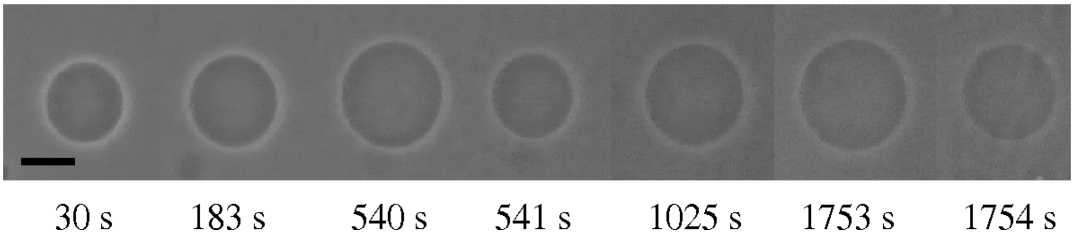

Figure 2. The sequence of the snapshots illustrates the growth and bursting of a vesicle (in glycerol, at OA concentration c = 0.1 mM). The length of the bar in the bottom left corner corresponds to 10 μm.

dx.doi.org/10.1021/jp404135g | J. Phys. Chem. B XXXX, XXX, XXX–XXX

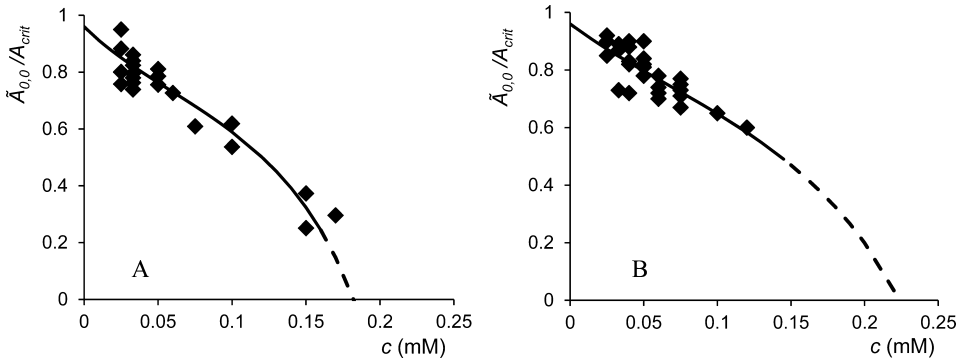

Figure 4. The measured ratio between $\tilde{A}_{0,0}$ (vesicle membrane area after the burst) and A_{crit} (vesicle membrane area before the burst) from 22 experiments with POPC vesicles (A) and 32 experiments with SOPC vesicles (B) are denoted with diamonds. The initial radii of the vesicles in these experiments ranged from 6 to 18 μm. The predictions of the model (next section, eq 6) are calculated (with setting $\gamma = 1.04$ and $\alpha = 12$) and fitted to the results for the ratio $\tilde{A}_{0,0}/A_{crit}$ with respect to the OA concentration (full lines; dashed parts of the curves denote the extrapolation according to the model), yielding the partition coefficients $K_{POPC} = 3400\ M^{-1}$ and $K_{SOPC} = 2500\ M^{-1}$, and the energy interaction parameters $\Delta w_{POPC} = -0.5kT$ and $\Delta w_{SOPC} = -0.4kT$. Only small variations (below 2%) in the values of the parameters are allowed to still obtain a suitable model fit of the measured data. However, it should be noted that the values of the parameters obtained are only indicative due to the approximative design of the model.

number of molecules of the first (PC, either POPC or SOPC) and the second (OA) component in the system, respectively, and a_1 and a_2 are the respective surface areas of the two types of molecules; the product N_1a_1 can be denoted as A_0, the initial membrane surface area of the vesicle. To describe the mixing of two membrane components we consider each of their molecules to occupy one site in a two-dimensional lattice and to interact with the neighboring molecules. To elucidate the principal mechanisms underlying the observed phenomena we will form the simplest possible model by assuming that the interactions between the neighbors in the lattice are mutually independent, that only the interactions between the neighboring molecules contribute to the energy of the system, and that each molecule in the membrane has an effective surface area (a_0). We describe the situation with three types of interaction-energy parameters $w_{i,j}$, where indices i and j become either a cipher 1 or 2, describing either the first or the second component of the system. They are $w_{1,1}$ for PC-PC, $w_{1,2}$ for PC-OA, and $w_{2,2}$ for OA-OA interactions. By adopting a "mean field" approximation, the enthalpy of a system is equal to the energy per molecule−molecule interaction between neighboring molecules, multiplied by the number of such interactions, where the number of all the interactions is calculated by summing over the product of the number of molecules of one type multiplied by the probability for the type of the neighboring molecule, $H = z^1/_2\Sigma_{i,j=1}^{2} w_{i,j}N_iX_j$; here, z stands for the number of the molecule's neighbors in the lattice, the factor of one-half corrects for the number of interactions that are accounted for in the summation, and X_1 and X_2 denote the mole fractions of the first and the second component, with $X_i = N_i/(N_1 + N_2)$. The entropy of the system is written as $S = -k(N_1 \ln X_1 + N_2 \ln X_2)$, where k is Boltzmann constant. Since there are only two components in the membrane we can substitute X_1 with $1 - X_2$ and write the expression for the free energy of the membrane with two mixed components as

$$G = \frac{z}{2}(w_{1,1}N_1 + N_2(1 - X_2)(2w_{1,2} - w_{1,1} - w_{2,2}) + N_2w_{2,2}) + kT(N_1 \ln(1 - X_2) + N_2 \ln X_2) + \frac{\kappa(A - \widetilde{A_0})^2}{2\widetilde{A_0}} \quad (2)$$

In the equilibrium, the OA molar ratio reaches the value where the chemical potential of fatty acid in the suspension ($\mu_s = \mu_0 + kT \ln c/c_0$, where c is the concentration of the FAs in the suspension and μ_0 and c_0 are constants) is equal to its value in the membrane ($\mu_m = \partial G \partial N_2$):

$$\mu_0 + kT \ln \frac{c}{c_0} = \frac{z}{2}(1 - X_2)^2(2w_{1,2} - w_{1,1} - w_{2,2}) + \frac{z}{2}w_{2,2} + kT \ln X_2 - \frac{\kappa a_0(A^2 - \widetilde{A_0}^2)}{2\widetilde{A_0}^2} \quad (3)$$

To make the relation between the OA concentration in the membrane (X_2) and in the bulk solution (c) more transparent, we rewrite this expression (eq 3) into a more compact form:

$$\ln \frac{X_2}{Kc} = \alpha\left(\left(\frac{A}{\widetilde{A_0}}\right)^2 - 1\right) - X_2(X_2 - 2)\frac{\Delta w}{kT} \quad (4)$$

where the parameter K ($K = (1/c_0)e^{(\mu_0 - \Delta w')/kT}$, with $\Delta w' = z(2w_{1,2} - w_{1,1})/2$) represents the partition coefficient of OA into an unstrained membrane of a PC GUV at small OA concentrations (at low OA molar ratio in the membrane, $X_2 = 1$), α stands for $\kappa a_0/2kT$, and $\Delta w = z(2w_{1,2} - w_{1,1} - w_{2,2})/2$ denotes an energy interaction parameter. Here, the characteristics of the model can be deduced more clearly: at low bulk OA concentrations, in a relaxed membrane, where A equals $\tilde{A}_0$, the partition coefficient (K) relates the amount of the partitioned OA molecules to a given bulk OA concentration ($X_{2,0} = Kc$). As in this case the equilibrium number of partitioned OA molecules is low compared to the number of the PC molecules in the GUV membrane, the molar ratio of the OA in the membrane can be obtained from $X_{2,0} \approx N_2/N_1$. When the membrane is strained, the X_2 ratio can be determined from eq 4 where within our simple model the relaxed membrane surface area can be expressed as $\tilde{A}_0 = A_0/(1 - X_2)$. At still low number of intercalated OA molecules in the membrane only the first term on the right-hand side accounts for the ratio of the strained and the relaxed surface areas ($A/\tilde{A}_0$). When the membrane is strained and significant numbers of OA molecules have partitioned into the membrane, beside the parameter α

dx.doi.org/10.1021/jp404135g | J. Phys. Chem. B XXXX, XXX, XXX−XXX

also the interactions between the OA molecules, accounted for by the parameter Δw, become important.

The membrane straining has a limit at a critical strain of the membrane, whereupon the vesicle bursts. For the PC membranes it was shown that the critical strain is reached when the difference between the actual membrane surface area A and the relaxed membrane surface area $\tilde{A}_0$ exceeds a certain maximum value.[25] Equation 4 can be used to find the ratio of the intercalated OA for a given c just before the vesicle bursting by taking for the ratio $A/\tilde{A}_0$ the material constant measuring the ratio between the surface areas of the critically strained membrane and the relaxed membrane with intercalated OA molecules $\gamma = A_{crit}/\tilde{A}_{0,crit}$):

$$\ln \frac{X_{2,crit}}{Kc} = \alpha(\gamma^2 - 1) - X_{2,crit}(X_{2,crit} - 2)\frac{\Delta w}{kT} \quad (5)$$

To compare the predictions of the model to the experimental results (the $\tilde{A}_{0,0}/A_{crit}$ ratio, Figure 4), eq 5 can be solved iteratively to obtain the OA molar ratio in the critically strained membrane ($X_{2,crit}$). We relate the calculated OA molar ratio to the relaxed membrane area $\tilde{A}_{0,crit} = A_0/(1 - X_{2,crit})$ at the moment of the burst and therefrom to the critically strained membrane area $A_{crit} = \gamma\tilde{A}_{0,crit} = \gamma A_0/(1 - X_{2,crit})$, while the expression for the membrane area increase due to the fatty acid intercalation into the membrane in the absence of membrane stretching is $\tilde{A}_{0,0} = A_0/(1 - X_{2,0}) = A_0/(1 - Kc)$. Then we can determine the ratio between the relaxed membrane after the burst ($\tilde{A}_{0,0}$) and the critically strained membrane area just before the burst (A_{crit}):

$$\frac{\tilde{A}_{0,0}}{A_{crit}} = \frac{(1 - X_{2,crit})}{\gamma(1 - Kc)} \quad (6)$$

After setting the values for the parameters γ, α, and K, this result (eq 6) can be compared to the measured value of the $\tilde{A}_{0,0}/A_{crit}$ ratio at a given OA concentration (Figure 4). The value for the parameter γ is set according to the reference for the critical strain for PC membranes ($\gamma = 1.04$).[25] The estimates for the area expansivity modulus κ for various PC membranes ($\kappa \approx 200$ mN/m)[26] and for the surface area-per-molecule a_0 (values for the surface areas of OA and PC molecules imply a_0 to be between 0.32 and 0.68 nm^2)[8,27,28] yield for the parameter α ($\alpha = \kappa a_0/2kT$) the values between 8 and 16. With the α value within the relevant interval we determine the parameter K for the described OA-PC system by fitting the model results to the initial slope of the curve through the measured data (Figure 4), as at low OA concentrations (with $X_2 \ll 1$) the initial slope of the curve describing the membrane surface area ratio ($\tilde{A}_{0,0}/A_{crit}$) after and before the burst with respect to the OA concentration is $d(\tilde{A}_{0,0}/A_{crit})/dc = K\{1 - \exp[\alpha(\gamma^2 - 1)]\}/\gamma)$. In the applied approximative model, multiple pairs of the parameter values K and α account for the same result regarding the initial slope, and the estimated interval of the values for α therefore yields the width of the estimated interval for the parameter K values (Figure 5).

The shape of the curve at higher OA concentrations depends also on the energy interaction parameter Δw, which is estimated from the best-fit of the model results to the data (Figure 4). By applying these parameters (the chosen pair of K and α, and the parameter Δw) for the whole span of OA concentrations this procedure yields a description of the vesicle membrane area characteristics at different concentrations of OA (as shown in Figure 4).

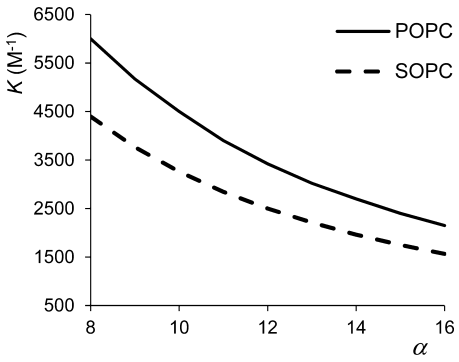

Figure 5. Values of the parameters K and α accounting for the same initial slopes of the curves describing the $\tilde{A}_{0,0}/A_{crit}$ ratio with respect to the increasing c as shown in Figure 4, for POPC and SOPC vesicles. A relevant interval for the parameter α is based on the estimates for the PC and OA molecules surface areas.

3.2.2. The Dynamics of the Swelling–Burst Cycle. Vesicle swelling, as shown in Figure 1, can be described by the permeation of glycerol and the accompanying osmotic flow of water into the interior of the vesicle. Membrane permeability for sucrose is much lower, and on the time scale relevant for this experiment, the membrane can be treated as impermeable for sucrose. The driving force for the vesicle swelling is the concentration difference for the permeable solute (in our case glycerol):

$$\frac{dn_g}{dt} = PA\left(c_{g,o} - \frac{n_g}{V}\right) \quad (7)$$

where n_g is the amount of glycerol inside the vesicle, P is the permeability of the vesicle membrane for glycerol, A is the membrane area, $c_{g,o}$ is the invariable molar concentration of glycerol in the vesicle exterior, and V is the vesicle volume. Since the permeability of the membrane for water is much higher than its permeability for glycerol,[29] we can assume that enough water permeates through the membrane almost instantaneously to keep the osmotic pressure inside the vesicle equal to the osmotic pressure outside the vesicle at all times:

$$RT\frac{n_g + n_s}{V} = RTc_{g,o} \quad (8)$$

Here, n_s is the amount of sucrose (the impermeable solute) inside the vesicle (due to the initial osmotic balance, $n_s = c_{g,o}V_0$). As the permeability of the membrane for sucrose is much lower than its permeability for glycerol, we can assume that the amount of sucrose remains constant until the vesicle bursts, $dn_s/dt = 0$. With a time derivative of eq 8 and by taking into account the spherical geometry of the treated system, we can rewrite eq 7 into a differential equation for the vesicle radius r:

$$\frac{dr}{dt} = P\left(\frac{r_0}{r}\right)^3 \quad (9)$$

where r_0 is the radius of the initial vesicle. The increase in the volume of the vesicle due to osmotic swelling is quantified by measuring the changes in the vesicle radius (Figure 1), which can be fitted with the solution of eq 9 for r, $r(t) = r_0(1 + 4Pt/r_0)^{1/4}$, to obtain the estimate for the membrane permeability for glycerol. The following values for P were obtained when comparing the data from Figure 1 with the predictions of the model: 3.5×10^{-8} m/s (0.05 mM OA), 1.9×10^{-8} m/s (0.10

dx.doi.org/10.1021/jp404135g | J. Phys. Chem. B XXXX, XXX, XXX–XXX

mM OA), 2.4×10^{-8} m/s (0.15 mM OA), and 2.6×10^{-8} m/s (0.20 mM OA).

At low OA concentrations the phenomenon of vesicle bursting has to be considered when regarding the membrane permeability for glycerol. When the membrane of the vesicle becomes critically strained due to the osmotic swelling, the vesicle bursts and ejects a part of its volume, whereupon the membrane reseals, with its surface area and the vesicle volume returning to their respective initial values. After the burst the process of osmotic swelling continues, which causes the bursts to occur periodically (Figures 2 and 3). With the assumption that the membrane is not permeable for sucrose molecules, we can consider the amount of sucrose inside the vesicle to decrease exclusively during the ejection of a small volume of the inner solution for the duration of the burst, by which the partial sucrose concentration does not change. The amount of sucrose inside the vesicle can thus be calculated after each of the periodical bursts (written below for the first, second, and nth burst):

$$\begin{aligned} n_{s,0} &= c_{s,0}V_0 = c_{s,1}V_{crit} \\ n_{s,1} &= c_{s,1}V_0 = c_{s,2}V_{crit} \\ &\cdots \\ n_{s,n} &= c_{s,n}V_0 = c_{s,n+1}V_{crit} \end{aligned} \tag{10}$$

where $n_{s,n}$ and $c_{s,n}$ refer to the amount and the partial molar concentration of sucrose in the vesicle after the nth burst, and V_{crit} is the volume of a critically strained vesicle. When describing the dynamics of the swelling–burst cycle we can use the relations from eq 10 and express $c_{s,n} = (V_0/V_{crit})^n c_{s,0}$, wherefrom a corresponding amount of sucrose inside the vesicle $n_{s,n}$ can be accounted for after each burst. Increasing the radius of the vesicle between two consecutive bursts (nth and (n +1)th burst) can be accomplished by generalizing the solution of eq 9:

$$(r(t))_n = r_0\left(1 + \left(\frac{V_0}{V_{crit}}\right)^n \frac{4Pt}{r_0}\right)^{1/4} \tag{11}$$

In the time interval $\Delta t_{1,2}$ between the first and the second burst, vesicle radius rises from its relaxed value r_0 to its critically strained value r_{crit} and for each vesicle, we can find the time interval between the two bursts from eq 11, expressed by the ratio between the area of a critically strained vesicle and the area of a relaxed vesicle:

$$\frac{\Delta t_{1,2}}{r_0} = \frac{1}{4P}\left(\left(\frac{A_{crit}}{\tilde{A}_{0,0}}\right)^2 - 1\right)\left(\frac{A_{crit}}{\tilde{A}_{0,0}}\right)^{3/2} \tag{12}$$

When the OA molar ratio in the membrane ($X_{2,crit}$) is determined at the moment of the burst (eq 5) and from there the $A_{crit}/\tilde{A}_{0,0}$ ratio calculated, we can resolve the $\Delta t_{1,2}$ interval at a given OA concentration. The calculated time intervals can be compared to the measured time intervals between the first two successive bursts (Figure 6) for each vesicle with initial radius r_0 to obtain an estimate on the adjustable parameter for membrane permeability for glycerol (P).

The increasing of the $A_{crit}/\tilde{A}_{0,0}$ ratio with the OA concentration (eq 6) underlays the increasing of the $\Delta t_{1,2}$ interval between the bursts. As demonstrated in Figure 6, the prediction of eq 12 corresponds to the experimental data when

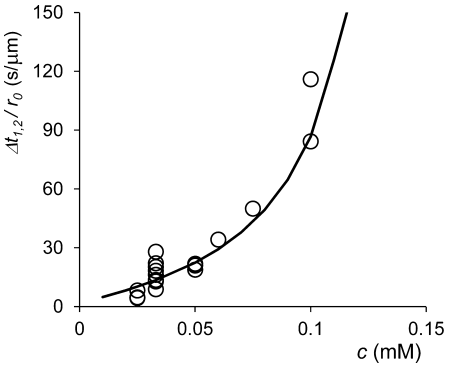

Figure 6. The measurements of the time intervals between the first and the second burst divided by the initial radius ($\Delta t_{1,2}/r_0$) of the vesicle in dependence on the OA concentration in the bulk solution (circles). The prediction of the model is shown (full line) for the best-fit value of membrane permeability for glycerol ($P = 1.2 \times 10^{-8}$ m/s).

the value for P equals 1.2×10^{-8} m/s, which is slightly lower than the results of the membrane permeability tracking with eq 9 (Figure 1). For each vesicle the characteristic time in which the vesicle volume doubles due to the permeation of glycerol can be determined as $\tau \approx 0.38 r_0/P$, meaning that we can estimate the volume of a vesicle with an initial radius $r_0 = 10$ μm to be doubled in ~5 min.

4. DISCUSSION

The lipid vesicles have been established as a convenient model for the prebiotic vesicles and a system for studying the ability of such entities to self-reproduce.[2,3] Since fatty acids as the simplest amphiphilic molecules can partition between the solution and the lipid aggregates, they are probable constituents of the prebiotic vesicle membranes[22] and have been shown to increase the vesicle surface area.[13] It has been suggested that self-reproduction of the vesicles is viable when the properties of the membrane are interrelated in a way that enables the growth of both the surface area of the membrane and the volume of the vesicle at the same time.[30] For a better insight into a general behavior of such systems we have designed an experiment in which the oleic acid molecules intercalate into the membrane of the vesicle, increasing its surface area, with the concomitant glycerol inflow that is osmotically increasing the volume of the vesicle. Applying the osmotic inflation of the vesicles also made it possible to sustain their spherical geometry, and consequently enabled us to determine the changes in the surface area of the vesicle and to quantify the partitioning of OA into the POPC (SOPC) membranes. At lower OA concentrations the consecutive bursting of the vesicles was observed where in one cycle the vesicle was swelling and the membrane strain was increasing up to a critical value, whereupon the membrane was relaxed by a burst for its surface area to attain the initial value, with the cycles repeating periodically (Figures 2 and 3). At higher OA concentrations, but still below the critical aggregation concentration for OA, the vesicles were swelling continuously, without the bursting in-between. In this section we will discuss the process of the vesicle bursting and thence estimate the energy-interaction constants, the critical OA concentration to allow for the continuous growth of the vesicles without bursting, and comment on the estimated values of the membrane permeability for glycerol.

In the process of swelling at low OA concentrations the vesicle radius increases considerably between the bursts, but the

dx.doi.org/10.1021/jp404135g | J. Phys. Chem. B XXXX, XXX, XXX–XXX

vesicle size after a burst coincides with its initial size. As oleic acid is much more soluble than phospholipids, the amount of the PC molecules in the solution is negligible, and it can be concluded that the vesicle area during the swelling stage increases due to the incorporation of the oleic acid molecules into the membrane, and that at the burst all the oleic acid being accumulated during the growth phase due to membrane strain is dissolved, while all the phospholipid remains in the membrane. The observed phenomenon is interpreted within the framework of a model which takes into account that the fatty acid partitioning into the phospholipid membrane depends on the stretching energy of the membrane. During the swelling stage, it is energetically favorable for the oleic acid molecules to intercalate into the membrane, since in this way they reduce the membrane stretching energy. At the moment of the burst the tension of the membrane abruptly drops to zero, and the energy requirement for the oleic acid molecules in the membrane vanishes. Upon membrane resealing and the subsequent start of a new swelling cycle, oleic acid starts to intercalate into the stretched membrane again.

Due to the spherical geometry of the vesicles we were able to determine the membrane surface area increase during the swelling stage, wherefrom we have deduced the estimates for the partition coefficients K_{POPC} = 3400 M^{-1} and K_{SOPC} = 2500 M^{-1} (Figure 4) for the OA molecules partitioning into POPC and SOPC membranes, respectively. The difference between the partition coefficients for the two types of membranes exhibits the same trend as the area expansivity modulus κ measurements, since it was found that κ for SOPC (κ = 290 mN/m)[31] is somewhat higher than for the POPC membrane (κ = 227 mN/m),[32] making it energetically more demanding for SOPC membranes to accommodate the incorporating OA molecules. Furthermore, it can be noted that the values of the partition coefficients K_{PC} for OA molecules into PC membranes are larger than the value of the partition coefficient for OA molecules into the membranes of the oleate vesicles K_{OA}, estimated from the relation with critical aggregation concentration for OA ($cac \cdot K_{OA} \approx 1$);[33] for example, the assessment for cac ≈ 0.5 mM[2] yields $K_{OA} \approx 2000\ M^{-1}$. The difference between K_{PC} and K_{OA} emphasizes that there is an energy difference between the case when OA molecules intercalate in-between the PC molecules ($K_{PC} = (1/c_0)\, e^{(\mu_0 - \Delta w_I)/kT}$), and the case when OA molecules intercalate in-between the neighboring OA molecules with ($K_{OA} = (1/c_0)\, e^{(\mu_0 - z w_{22}/2)/kT}$). The unknown constants μ_0 and c_0 cancel out when the expressions for the respective partition coefficients are divided, wherefrom we are able to obtain the estimate for $\Delta w/kT = -\ln(K_{PC}/K_{OA})$, yielding the energy parameter value Δw to be around $-0.5kT$ for PC membranes. This is close to the values obtained from the procedure of fitting the model predictions to the experimental results (Figure 4), indicating the consistency of the estimate for cac in our system (~0.5 mM). The discrepancy with other reported values for cac[21,22] may be ascribed to the large sensitivity of this quantity to the experimental conditions like pH and ionic strength,[2,21] or even to the method applied.[34]

The value of Δw affects the shape of the model curve (Figure 4) at higher OA concentrations and it is observed that by the model prediction the curve intersects with the x-axis. Above this value of OA concentration no vesicle bursts are expected to occur and are also not detected. The intersection with the x-axis indicates that ratio $\tilde{A}_{0,0}/A_{crit} = 0$, at which, as implied by eq 6, the ratio of OA in the membrane should reach 1 ($X_2 = 1$). With continuous glycerol inflow the membrane is straining continuously and new OA molecules are incorporated into the membrane; however, because of the POPC molecules already present in the membrane, the $X_2 = 1$ ratio cannot be achieved. In addition to the membrane stretching, the presence of POPC molecules in the membrane thus provides a further reason for the enhanced partitioning of the OA molecules into the vesicle membranes. The continuous partitioning is energetically favorable and at high bulk OA concentrations prevents the membrane from straining critically, though according to the referential experiments the concentrations are still below the critical aggregation concentration value (cac).[2,13] Comparing POPC and SOPC vesicles, for POPC membranes the curve intersects with the x-axis at lower OA concentrations, which can also be understood by the lower κ value (Figure 4A,B).

While the presented model for strain-enhanced partitioning of OA into the membrane provides a plausible explanation for the experimental set of data, some simplifications made may be considered as the limitations of the model. In several ways, the model was simplified by taking an effective constant value where a dependence on membrane composition might be expected: (a) the surface areas of both the POPC (SOPC) and OA molecules were taken to equal an effective surface area of a molecule in a lattice ($a_1 = a_2 = a_0$), (b) the critical membrane strain was set to 4% increase over the initial surface area of the relaxed membrane before the osmotic swelling ($\tilde{A}_0$) for the whole span of OA concentration fractions in the membrane, and (c) the membrane stretching modulus κ is also a quantity that may change with the membrane composition. The values of the above parameters were taken from the interval of the expected values for these quantities. Despite the approximations made, the described model qualitatively explains the vesicle behavior.

On the subject of the membrane permeability, one of the simplifications made was in disregarding that the vesicles transferred into the solution with OA and glycerol are not spherical, which causes a systematic underestimation of the membrane permeability for glycerol (P) in cases when the vesicles are in fact oblate. A suitable parameter to assess the extent by which they depart from the spherical shape is the reduced volume (v), the quotient of the vesicle volume (V), and the volume of a sphere with an area equal to the area of the vesicle membrane ($A^{3/2}/6\pi^{1/2}$, with A being the membrane surface area), which ranges from 0 to 1 and equals 1 for a sphere. There are two reasons for the reduced volume to be initially less than 1: first, we may already have started with a vesicle that was flaccid, i.e., not perfectly spherical, and therefore its reduced volume (v_0) was less than 1, and second, after the transfer, vesicle membrane area increases rapidly due to the intercalation of oleic acid, thus diminishing the reduced volume even further by making the vesicle more flaccid ($v_{OA} = (A_0/\tilde{A}_{0,0})^{3/2} = (1 - Kc)^{3/2}$). The initial reduced volume v_i is the product of both contributions, $v_i = v_0 v_{OA}$. For an accurate calculation of membrane permeability for glycerol we should have known the initial reduced volume of the vesicle. Based on our experience with GUVs made by the electroformation method, we can estimate $0.95 < v_0 < 1$. The glycerol molar ratio inside the vesicle before the onset of the swelling stage can be determined from $X_{g,0} = 1 - v_0 v_{OA}$, implying that the glycerol concentration gradient across the membrane is smaller than assumed in formulating eq 7, and that therefore the permeability of the membrane for glycerol is somewhat larger

dx.doi.org/10.1021/jp404135g | J. Phys. Chem. B XXXX, XXX, XXX−XXX

than estimated. By taking into account the flaccidity of the vesicles, which was omitted in the calculations (eqs 7−12) for the sake of clarity, the upper limit estimate for P is corrected to 4.3×10^{-8} m/s, which is in agreement with the previous studies on the PC-membrane permeability for glycerol.[20,35−38]

5. CONCLUSIONS

An experiment is presented in which the lipid composition of the membrane of the giant vesicle was changing due to the partition of oleic acid (OA) from the outer solution into the osmotically strained membrane. To describe the observed phenomena we constructed a model that explains the changes of the volume and the surface area of the membrane in the observed vesicles in terms of energetically most favorable outcomes of membrane−OA interactions. The presented model provides a plausible explanation of the crucial mechanisms governing the behavior of the two-component system of the OA/POPC (SOPC) vesicles, and demonstrates that the OA partitioning into the membrane of the vesicle is enhanced when the membrane is strained as the elastic energy of the membrane is diminished when additional molecules incorporate into the membrane. The partition coefficient K for OA partitioning into GUV−POPC (SOPC) membranes, and the permeability constant P for glycerol permeation through POPC−membranes were estimated and found to be consistent with the findings in the literature.

■ AUTHOR INFORMATION

Corresponding Author

*Tel: 00 386 1 543 7600. E-mail: mojca.mally@mf.uni-lj.si.

Notes

The authors declare no competing financial interest.

■ ACKNOWLEDGMENTS

We thank Prof. Peter Walde for a thoughtful reading of the manuscript and his useful comments. This work was supported by the Slovenian Research Agency through grants J3-2268 and P1-0055.

■ REFERENCES

(1) McArthur, M. J.; Atshaves, B. P.; Frolov, A.; Foxworth, W. D.; Kier, A. B.; Schroeder, F. Cellular Uptake and Intracellular Trafficking of Long Chain Fatty Acids. *J. Lipid Res.* **1999**, *40*, 1371−1383.

(2) Walde, P.; Wick, R.; Fresta, M.; Mangone, A.; Luisi, P. L. Autopoietic Self-Reproduction of Fatty Acid Vesicles. *J. Am. Chem. Soc.* **1994**, *116*, 11649−11654.

(3) Hanczyc, M. M.; Fujikawa, S. M.; Szostak, J. W. Experimental Models of Primitive Cellular Compartments: Encapsulation, Growth, and Division. *Science* **2003**, *302*, 618−622.

(4) Hanczyc, M. M.; Szostak, J. W. Replicating Vesicles as Models of Primitive Cell Growth and Division. *Curr. Opin. Chem. Biol.* **2004**, *8*, 660−664.

(5) Briers, Y.; Walde, P.; Schuppler, M.; Loessner, M. J. How Did Bacterial Ancestors Reproduce? Lessons from L-Form Cells and Giant Lipid Vesicles: Multiplication Similarities between Lipid Vesicles and L-Form Bacteria. *Bioessays* **2012**, *34*, 1078−1084.

(6) Errington, J. L-Form Bacteria, Cell Walls and the Origins of Life. *Open Biol.* **2013**, *3*, 120143.

(7) Lonchin, S.; Luisi, P. L.; Walde, P.; Robinson, B. H. A Matrix Effect in Mixed Phospholipid/Fatty Acid Vesicle Formation. *J. Phys. Chem. B* **1999**, *103*, 10910−10916.

(8) Kleinfeld, A. M.; Chu, P.; Romero, C. Transport of Long-Chain Native Fatty Acids across Lipid Bilayer Membranes Indicates That Transbilayer Flip-Flop Is Rate Limiting. *Biochemistry* **1997**, *36*, 14146−14158.

(9) Høyrup, P.; Davidsen, J.; Jørgensen, K. Lipid-Membrane Partitioning of Lysolipids and Fatty Acids: Effect of Membrane Phase Structure and Detergent Chain Length. *J. Phys. Chem. B* **2001**, *105*, 2649−2657.

(10) Hąc-Wydro, K.; Wydro, P. The Influence of Fatty Acids on Model Cholesterol/Phospholipid Membranes. *Chem. Phys. Lipids* **2007**, *150*, 66−81.

(11) Hamilton, J. A.; Johnson, R. A.; Corkey, B.; Kamp, F. Fatty Acid Transport: The Diffusion Mechanism in Model and Biological Membranes. *J. Mol. Neurosci.* **2001**, *16*, 99−108.

(12) Kampf, J. P.; Kleinfeld, A. M. Is Membrane Transport of FFA Mediated by Lipid, Protein, or Both? An Unknown Protein Mediates Free Fatty Acid Transport across the Adipocyte Plasma Membrane. *Physiology* **2007**, *22*, 7−14.

(13) Peterlin, P.; Arrigler, V.; Kogej, K.; Svetina, S.; Walde, P. Growth and Shape Transformations of Giant Phospholipid Vesicles upon Interaction with an Aqueous Oleic Acid Suspension. *Chem. Phys. Lipids* **2009**, *159*, 67−76.

(14) Evans, E.; Rawicz, W.; Hofmann, A. F. In *Bile Acids in Gastroenterology: Basic and Clinical Advances*; Hofmann, A. F., Paumgartner, G., Stiehl, A., Eds.; Kluwer Academic Publishers: Lancaster, U.K., 1995; pp 59−68.

(15) Zhelev, D. V. Material Property Characteristics for Lipid Bilayers Containing Lysolipid. *Biophys. J.* **1998**, *75*, 321−330.

(16) Angelova, M. I.; Dimitrov, D. S. Liposome Electro Formation. *Faraday Discuss. Chem. Soc.* **1986**, *81*, 303−311.

(17) Mally, M.; Majhenc, J.; Svetina, S.; Žekš, B. Mechanisms of Equinatoxin II−Induced Transport through the Membrane of a Giant Phospholipid Vesicle. *Biophys. J.* **2002**, *83*, 944−953.

(18) Dimova, R.; Aranda, S.; Bezlyepkina, N.; Nikolov, V.; Riske, K. A.; Lipowsky, R. A Practical Guide to Giant Vesicles. Probing the Membrane Nanoregime via Optical Microscopy. *J. Phys.: Condens. Matter* **2006**, *18*, S1151−S1176.

(19) Döbereiner, H.-G.; Evans, E.; Kraus, M.; Seifert, U.; Wortis, M. Mapping Vesicle Shapes into the Phase Diagram: A Comparison of Experiment and Theory. *Phys. Rev. E* **1997**, *55*, 4458−4474.

(20) Peterlin, P.; Jaklič, G.; Pisanski, T. Determining Membrane Permeability of Giant Phospholipid Vesicles from a Series of Videomicroscopy Images. *Meas. Sci. Technol.* **2009**, *20*, 055801−1−7.

(21) Chen, I. A.; Szostak, J. W. Membrane Growth Can Generate a Transmembrane pH Gradient in Fatty Acid Vesicles. *Proc. Natl. Acad. Sci. U.S.A.* **2004**, *101*, 7965−7970.

(22) Budin, I.; Szostak, J. W. Physical Effects Underlying the Transition from Primitive to Modern Cell Membranes. *Proc. Natl. Acad. Sci. U. S. A.* **2011**, *108*, 5249−5254.

(23) Smith, R.; Tanford, C. The Critical Micelle Concentration of L-α-Dipalmitoylphosphatidylcholine in Water and Water/Methanol Solutions. *J. Mol. Biol.* **1972**, *67*, 75−83.

(24) Kamp, F.; Zakim, D.; Zhang, F.; Noy, N.; Hamilton, J. A. Fatty Acid Flip-Flop in Phospholipid Bilayers Is Extremely Fast? *Biochemistry* **1995**, *34*, 11928−11937.

(25) Bloom, M.; Evans, E.; Mouritsen, O. G. Physical Properties of the Fluid Lipid-Bilayer Component of Cell Membranes: A Perspective. *Q. Rev. Biophys.* **1991**, *24*, 293−397.

(26) Allende, D.; Simon, S. A.; McIntosh, T. J. Melittin-Induced Bilayer Leakage Depends on Lipid Material Properties: Evidence for Toroidal Pores. *Biophys. J.* **2005**, *88*, 1828−1837.

(27) Koenig, B. W.; Strey, H. H.; Gawrisch, K. Membrane Lateral Compressibility Determined by NMR and X-Ray Diffraction: Effect of Acyl Chain Polyunsaturation. *Biophys. J.* **1997**, *73*, 1954−1966.

(28) Kučerka, N.; Tristram-Nagle, S.; Nagle, J. F. Structure of Fully Hydrated Fluid Phase Lipid Bilayers with Monounsaturated Chains. *J. Membr. Biol.* **2005**, *208*, 193−202.

(29) Walter, A.; Gutknecht, J. Permeability of Small Nonelectrolytes through Lipid Bilayer Membranes. *J. Membr. Biol.* **1986**, *90*, 207−217.

763 (30) Božič, B.; Svetina, S. Vesicle Self-Reproduction: The
764 Involvement of Membrane Hydraulic and Solute Permeabilities. *Eur.*
765 *Phys. J. E: Soft Matter Biol. Phys.* **2007**, *24*, 79−90.
766 (31) Rawicz, W.; Smith, B. A.; McIntosh, T. J.; Simon, S. A.; Evans,
767 E. Elasticity, Strength, and Water Permeability of Bilayers that Contain
768 Raft Microdomain-Forming Lipids. *Biophys. J.* **2008**, *94*, 4725−4736.
769 (32) Troiano, G. C.; Stebe, K. J.; Raphael, R. M.; Tung, L. The
770 Effects of Gramicidin on Electroporation of Lipid Bilayers. *Biophys. J.*
771 **1999**, *76*, 3150−3157.
772 (33) Israelachvili, J. N.; Mitchell, D. J.; Ninham, B. W. Theory of self-
773 assembly of hydrocarbon amphiphiles into micelles and bilayers. *J.*
774 *Chem. Soc.* **1976**, *72*, 1525−1568.
775 (34) Teo, Y. Y.; Misran, M.; Low, K. H.; Zain, S. Md. Effect of
776 Unsaturation on the Stability of C18 Polyunsaturated Fatty Acids
777 Vesicles Suspension in Aqueous Solution. *Bull. Korean Chem. Soc.*
778 **2011**, *32*, 59−64.
779 (35) Peterlin, P.; Arrigler, V. Electroformation in a Flow Chamber
780 with Solution Exchange as a Means of Preparation of Flaccid Giant
781 Vesicles. *Colloids Surf., B* **2008**, *64*, 77−87.
782 (36) Paula, S.; Volkov, A. G.; Van Hoek, A. N.; Haines, T. H.;
783 Deamer, D. W. Permeation of Protons, Potassium Ions, and Small
784 Polar Molecules through Phospholipid Bilayers as a Function of
785 Membrane Thickness. *Biophys. J.* **1996**, *70*, 339−348.
786 (37) Dordas, C.; Brown, P. H. Permeability of Boric Acid Across
787 Lipid Bilayers and Factors Affecting It. *J. Membr. Biol.* **2000**, *175*, 95−
788 105.
789 (38) Orbach, E.; Finkelstein, A. The Nonelectrolyte Permeability of
790 Planar Lipid Bilayer Membranes. *J. Gen. Physiol.* **1980**, *75*, 427−436.